JOC The Journal of Organic Chemistry

Article

pubs.acs.org/joc

Design Strategies for Shape-Persistent Covalent Organic Polyhedrons (COPs) through Imine Condensation/Metathesis

Yinghua Jin,[†] Athena Jin,[†] Ryan McCaffrey,[†] Hai Long,[‡] and Wei Zhang*[,†]

[†]Department of Chemistry and Biochemistry, University of Colorado, Boulder, Colorado 80309, United States

[‡]National Renewable Energy Laboratory, Golden, Colorado 80401, United States

Supporting Information

ABSTRACT: A series of dialdehyde compounds were synthesized and reacted with the complementary triamines (either planar or pyramidal with a 109.5° vertex) in a 3:2 ratio to explore the structural requirements on the building blocks for the successful construction of shape-persistent, covalent organic polyhedrons (COPs). Structural variations in the building blocks included the distance and angle between the two reactive sites (aldehyde or amine functional groups) and the absence/presence of solubilizing chains. Computer modeling was utilized to determine and compare the thermodynamic stabilities of some of these COP structures. Furthermore, gas adsorption studies were performed to explore the potential of these molecular cages for gas separation, particularly carbon capture, applications.

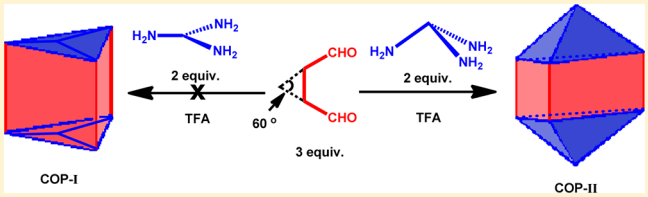

INTRODUCTION

In the past two decades, there has been emerging interest in synthetic molecular cages and their applications.[1−7] With the advent of supramolecular chemistry[2,3,6] and dynamic covalent chemistry,[8−11] chemists have been able to gain facile access to a wide variety of molecular cages, and significant advances have been made in exploring their applications in the area of molecular recognition,[2,5,12] chemical sensing,[13,14] catalysis,[15−18] and gas separation and storage.[19−21] To date, most molecular cages have been prepared through self-assembly process driven by metal−ligand coordination[3,4,22] or hydrogen bonding.[2,23−27] Chemically and thermally robust covalent organic polyhedrons (COPs) have also been prepared under dynamic conditions through imine,[21,28−34] borate,[35,36] disulfide,[37,38] and more recently, alkyne formation.[39,40] However, it still remains a challenge to synthesize COPs of precise dimensions and shape with surface functionalities, which is of great importance to tune the bulk material properties.

Our group has been interested in exploring the possibility of applying low-density COP[21,33] compounds and their cross-linked framework materials for gas separation,[41] especially for separation of CO_2/N_2. Extensive studies have been carried out on zeolites,[42,43] metal−organic frameworks (MOFs),[44−48] and covalent organic frameworks (COFs),[49−53] all well-established classes of porous materials, for gas separation and storage. However, not until recently have discrete organic cages been introduced as a viable class of novel porous materials.[19,21,31,33,54−56] Conventionally, the COPs are synthesized under irreversible reaction conditions, and usually very low overall yields are obtained, thus impeding their practical applications in gas adsorption/separation. Although recent advances in dynamic covalent chemistry, particularly imine condensation/metathesis reaction, has promised ready access to a variety of COPs, some fundamental questions still remain to be answered, such as what are the criteria for the selection of building blocks for successful cage formation, particularly for those shape-persistent, noncollapsible cages? Are there any requirements for the relative positions (e.g., angle, direction) of those functional groups in the building units? Is it necessary to install the solubilizing groups on the starting precursors? Will the selection of reaction medium affect the product formation? To gain better understanding on the design rules for COPs, a systematic study exploring the critical structural parameters determining the success in COP formation is highly desired. Design strategies for building blocks of noncovalent assemblies via metal coordination are well documented,[3,4,57] which paves the way for exploring the construction of 3-D COPs. Herein, we report the design and syntheses of a series of trigonal prismatic and football-shaped cage molecules through imine condensation/metathesis. Such systematic study explores the dependence of successful COP formation on certain important structural parameters and will shed some light on the rational design principle for construction of well-defined COP-based nanostructures. Additionally, **COP^{II}-20** showed a high ideal selectivity in adsorption of CO_2 over N_2 (80/1, mol/mol), thus representing another promising candidate material for carbon capture applications.

RESULTS

Syntheses of Dialdehyde and Triamine Building Blocks. Dialdehydes **1**−**7** and triamines **8** and **9** with different structural and geometrical features (angles and distances between the two functional moieties) were synthesized. The

Received: June 7, 2012
Published: August 21, 2012

dx.doi.org/10.1021/jo3011683 | J. Org. Chem. 2012, 77, 7392−7400

pyrene-based dialdehyde building blocks (**1**, **2a,b**) were synthesized from the 1,8-diethynylpyrene (**10**).[58] Sonogashira cross-coupling between **10** and several different aromatic halides afforded dialdehyde building blocks (**1**, **2a,b**, Scheme 1). For compound **2b**, the decynyl group was installed to

Scheme 1. Syntheses of Dialdehydes 1 and 2a,b

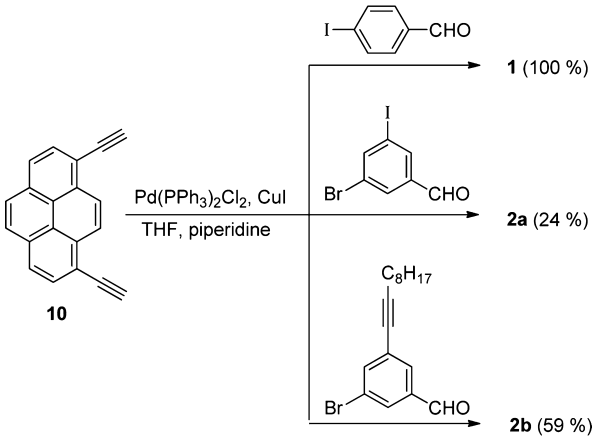

enhance the solubility of the precursor and intermediate oligomers. The tetraphenylmethane-based triamine building unit (**9**) was synthesized from the tricarboxylic acid **11**.[59] Esterification followed by Suzuki cross-coupling provided the tetradecyl-substituted trimethyl ester **13**. Hydrolysis, Curtius rearrangement, and subsequent amine deprotection provided triamine **9** (Scheme 2).

Scheme 2. Synthesis of Triamine 9

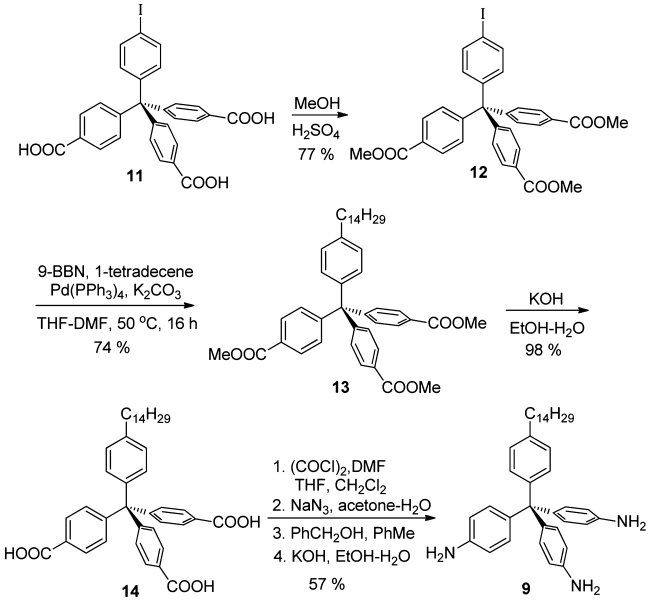

Syntheses of COPs. We tested various dialdehydes (**1**−**7**) with the angles between the two reactive aldehyde sites (in the same plane) ranging from 0° to 300° in imine condensation/metathesis reaction with triamines **8a**, **8b**, and **9** to investigate the design criteria for the building blocks that would lead to successful cage formations. The results are summarized in Table 1. In all the attempted syntheses of COPs, the imine condensation/metathesis was conducted at room temperature

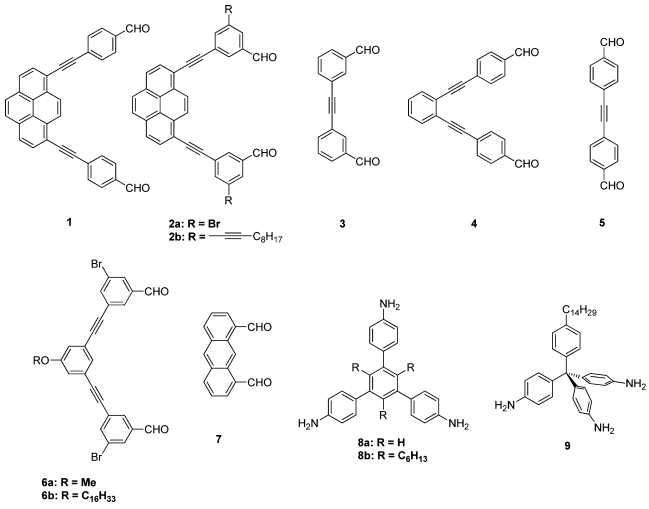

Table 1. Syntheses of COPs via Imine Condensation/Metathesis Followed by Reduction

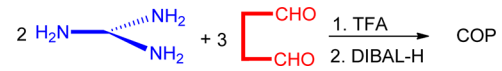

entry	triamine	dialdehyde	solvent	COP product[a]	yield[a,b]
1	**8b**	**1**	TCB	ND	NA
2	**8b**	**2a**	TCB	**COP^{I}-15a**	23
3	**8b**	**2b**	$CHCl_3$	**COP^{I}-15b**	83
4	**8b**	**3**	$CHCl_3$	ND	NA
5	**8b**	**4**	$CHCl_3$	ND	NA
6	**8b**	**5**	$CHCl_3$	ND	NA
7[d]	**8b**	**6a**	$CHCl_3$	**COP^{I}-16a**	21
8[d]	**8b**	**6b**	$CHCl_3$	**COP^{I}-16b**	46
9[d]	**8b**	**7**	$CHCl_3$	**COP^{I}-17a**	74
10[d]	**8a**	**7**	$CHCl_3$	**COP^{I}-17b**	75
11	**9**	**1**	TCB	**COP^{II}-18**	78
12	**9**	**2a**	TCB	**COP^{II}-19a/DT^{II}-19a**[c]	trace
13	**9**	**2b**	$CHCl_3$	**COP^{II}-19b/DT^{II}-19b**[c]	trace
14	**9**	**3**	$CHCl_3$	**COP^{II}-20**	31
15	**9**	**4**	$CHCl_3$	**COP^{II}-21**	94
16	**9**	**5**	$CHCl_3$	ND	NA
17	**9**	**6a**	$CHCl_3$	**COP^{II}-22**	11
18	**9**	**7**	$CHCl_3$	**COP^{II}-23**	69

[a]ND = not detected, NA = not applicable. [b]Isolated yield. [c]Species with molecular weight corresponding to COP^{II}/DT was observed on the MALDI mass spectra, [d]Previously described; see refs 21 and 33.

(rt) under acid catalysis. Previously, we used $Sc(OTf)_3$ as the imine metathesis catalyst.[21,33] However, we encountered some complications such as sluggish reactions with aged or different batches of $Sc(OTf)_3$ from various suppliers. We found a catalytic amount of trifluoroacetic acid (TFA) provides similar results as the fresh $Sc(OTf)_3$. In general, 3 equiv of dialdehydes (**1**−**7**) were reacted with 2 equiv of triamine (**8a** or **8b** or **9**) in $CHCl_3$ (or 1,2,4-trichlorobenzene) at room temperature under the catalysis of TFA. The concentrations of the triamine and dialdehyde building blocks are 3.0 and 4.5 mM, respectively. We found the concentration is important: high concentration leads to fast initial condensation to form insoluble intermediate oligomeric species; low concentration leads to very sluggish reaction. Upon formation of the imine-linked COPs, diisobutylaluminum hydride (DIBAL-H) was added as an efficient reducing agent to reduce the imine bonds to the amines at various temperatures.[60] Except for entries 1, 2, 6, 7,

dx.doi.org/10.1021/jo3011683 | J. Org. Chem. 2012, 77, 7392−7400

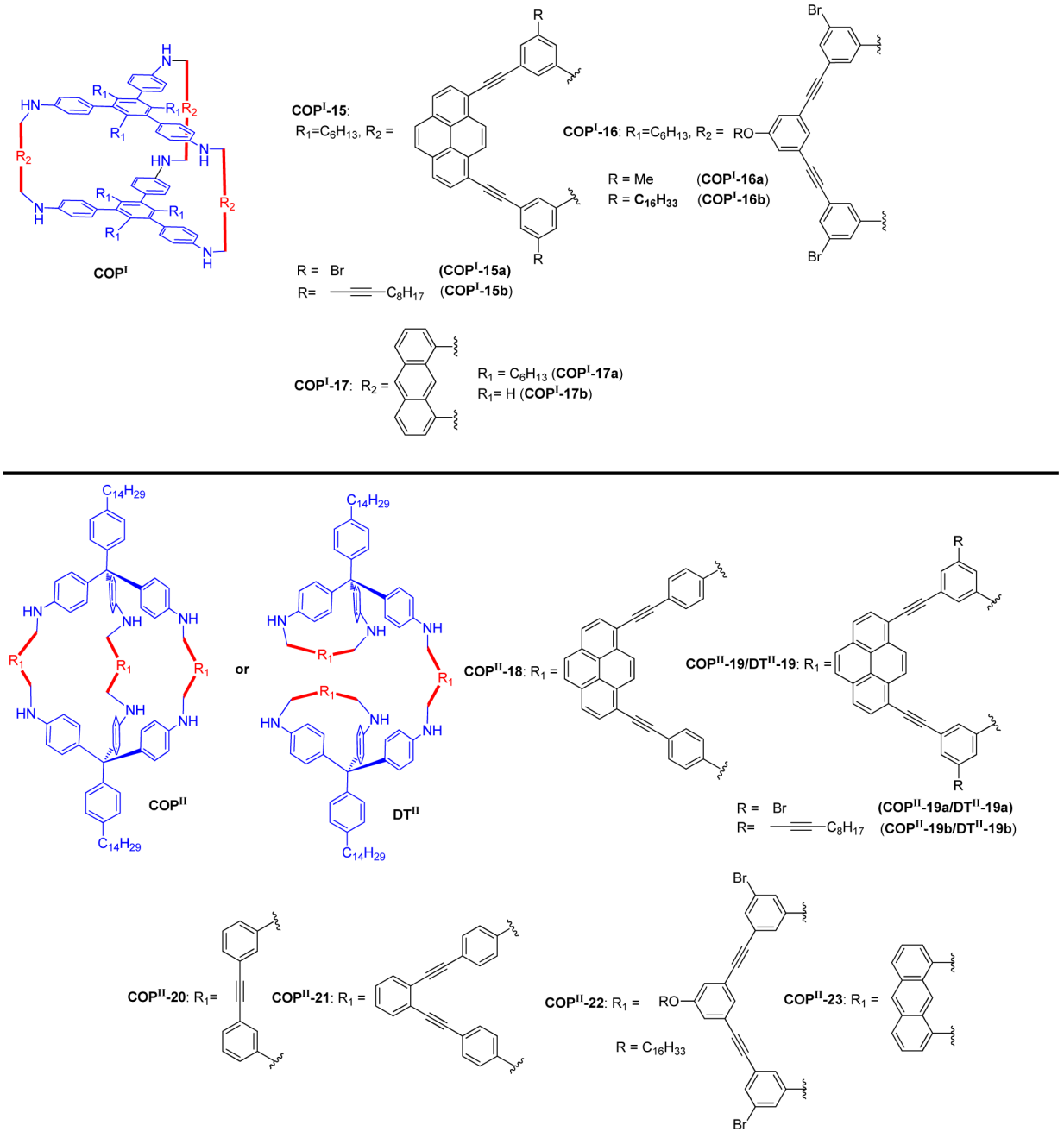

Figure 1. COP/DT structures observed in this study.

10, and 16, the reaction mixture stayed as a clear solution throughout the reaction. In all entries, no efforts were made to remove the condensation byproduct water, and we observed almost complete conversions of starting materials after 18−24 h. As shown in Table 1, we were able to isolate pure trigonal prisms (**COP^{I}-15a**, **COP^{I}-15b**, **COP^{I}-16a**, **COP^{I}-16b**, **COP^{I}-17a**, **COP^{I}-17b**, Figure 1) and elongated molecular triangular bipyramids (**COP^{II}-18**, **COP^{II}-20**, **COP^{II}-21**, **COP^{II}-22**, and **COP^{II}-23**) in various yield (11−94%). All COP products were purified by flash column chromatography and characterized by ^{1}H and ^{13}C NMR, GPC, and MALDI-MS (Supporting Information).

At the equilibrium, various intermediates were observed in the failed/low yielding syntheses of COPs. In entries 6 and 16, the imine condensation/metathesis provided mostly insoluble species, presumably higher molecular weight oligomers or polymers. Although the formation of a higher ordered dodecahedral imine-linked COP may be possible, we did not detect any species indicative of its presence in the MALDI-MS of the reduced reaction mixture. In entry 14, we observed I_2 as another major species in addition to the desired **COP^{II}-20**, with a trace amount of higher ordered polyhedron species (tetrahedron, or interlocked prism). Partially closed intermediates I_2 and I_3 (Figure 2) were observed as the major species in the MALDI-MS in entries 4 and 5 even after 3 days of reaction. Interestingly, in entry 1, we observed mono-triangle type intermediates I_5 and I_6 as the major species. Intermediates I_5 (predominant) and I_6 were also observed in entries 12 and 13 as the major species along with trace amount of the species with the correct m/z of the target COPs on MALDI-MS. Thus the species with the same m/z as the target COP observed in

dx.doi.org/10.1021/jo3011683 | J. Org. Chem. 2012, 77, 7392−7400

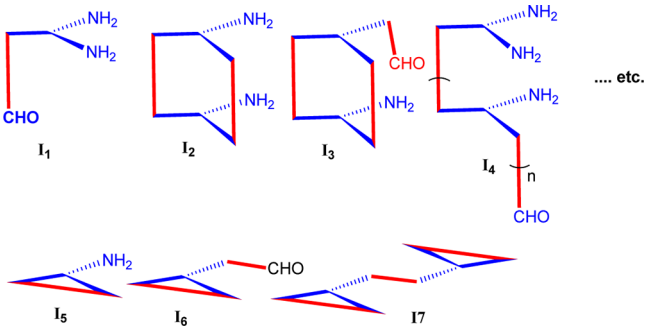

Figure 2. Possible intermediate structures along the pathway to COPs. Triamine building blocks are blue, and dialdehyde building blocks are red.

entry 12 and 13 are more likely I_7 type double triangle (DT) instead of the desired cage products. However, we were unable to isolate them and determine their structures.

Gas Adsorption Study. Previously we have reported the high selectivity of some COP^{I}s in adsorption of CO_2 over N_2.[21,33] Under the STP (1 bar, 20 °C) condition, cages **COP^{I}-16b**, **COP^{I}-17a**, and **COP^{I}-17b** showed a high selectivity of up to 138/1 (CO_2/N_2), thus showing great potential in carbon capture applications. The gas adsorption behavior of the elongated triangular bipyramidal cages (COP^{II}) containing the new pyramidal triamine building blocks (**9**) was investigated by using cage **COP^{II}-20** as a representative example. We measured the gas adsorption isotherms of amorphous desolvated sample of **COP^{II}-20** as previously described using the custom-built instrument for low-adsorption-capacity materials.[21,41] The gas adsorption isotherms (Figure 3) show an adsorption capacity

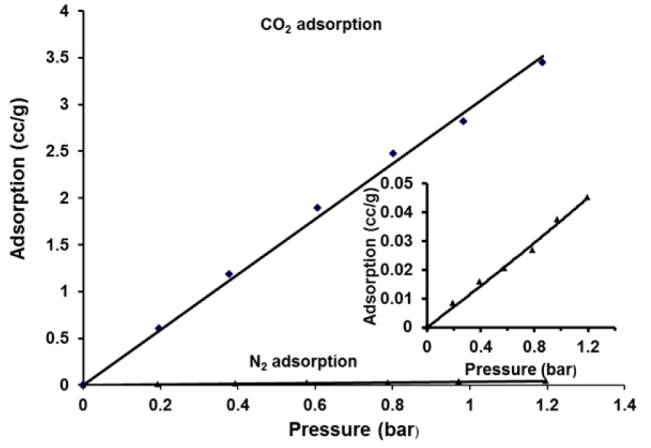

Figure 3. CO_2- and N_2-adsorption isotherms at 20 °C for **COP^{II}-20**. Inset: N_2-adsorption isotherm.

and CO_2/N_2 selectivity comparable to that of COP^{I} derivatives, with an adsorption capacity of 2.96 cc/g for CO_2 and 0.037 cc/g for N_2, resulting in an ideal adsorption selectivity of 80/1 under the STP condition.[61]

DISCUSSION

With the aim of constructing shape-persistent 3-D COPs, we selected building blocks containing rigid aromatic moieties in the backbone with a minimum number of saturated carbons. Owing to the rigidity of the building units, the shape of the self-assembled structure is largely determined by the geometrical and chemical information encoded into the building blocks. In the following discussions, we assume sp^3 hybridized carbons have bond angles of ~109.5° and sp^2 hybridized carbons have bond angles of ~120°. Planar (**8a** or **b**) triamines with 120° angle between any two amino groups were used in the assembly of trigonal prismatic cage (Scheme 3, I). Elongated triangular

Scheme 3. Schematic Presentation of the Covalent Assembly of Molecular Cages

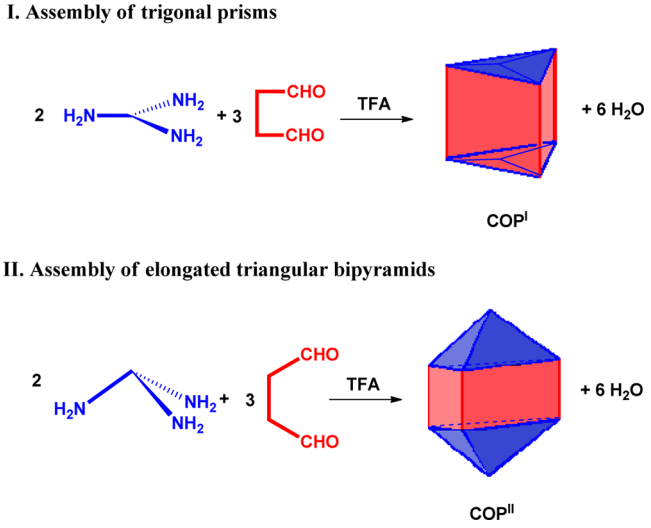

bipyramids are simple variations of triangular prisms, which could be easily assembled in a similar fashion by using a tritopic unit with 109.5° angle between the two adjacent amino groups as a vertex synthon. We selected pyramidal triamine (**9**) as the vertex directing the assembly of the proposed elongated triangular bipyramids (Scheme 3, II). The structural variations of the dialdehyde building blocks include the absence/presence of solubilizing chains, the distance and the angle between the two aldehyde groups, which enabled us to determine what parameters are critical for successful cage formation. The isolated yields of COPs were determined after reduction of imine-linked COPs to more robust amine-linked ones. The yields were used as an approximate indicator of the actual degree of imine-linked cage formation, which was also supported by the GPC characterization of the crude amine cage product mixtures (Supporting Figures S3–S4)

Geometric Parameters of Building Blocks: Relative Orientation of Reactive Sites and Conformational Rigidity. It should be noted that imine bond formation prefers *trans* conformation and is rather rigid. Therefore, it can be considered as "quasi-linear", similar to a metal–ligand dative bond. It appears that dynamic covalent approach and noncovalent assembly via metal coordination share similar requirements on building block geometries for the successful COP formation. "Matched" orientation (allowing the formation of low- or no-strain structures) of the functional groups and rigidity (enhancing directional effect through "pre-organization") of building blocks are desired for high-yielding synthesis of COPs.

Previously we have reported the successful cage formation by reacting the planar triamine (**8b**) and the anthracene-based dialdehyde (**7**) in chloroform at room temperature.[33] After the hydride reduction, the target amine cage (**COP^{I}-17a**) was obtained with a 74% isolated yield. In order to construct COPs

dx.doi.org/10.1021/jo3011683 | J. Org. Chem. 2012, 77, 7392–7400

Table 2. Energy Calculations (kcal/mol) of the Intermediates and COPs

entry	triamine (III)	dialdehyde (IV)	III + IV	I_5	$I_5 + I_5 + IV$	I_4 ($n = 2$)	$I_4 + IV$	I_2	$I_2 + IV$	COP
1	37.6[b]	24.8	62.4	69.4	163.6	95.6	120.4	113.2	138.0	139.6
2/3[a]	37.6[b]	24.5	62.1	65.8	156.1	99.8	124.3	97.0	121.5	117.6 (**COP^{I}-15**)
4	37.6[b]	10.1	47.7	59.3	128.7	79.2	89.3	84.1	94.2	106.4
5	37.6[b]	14.5	52.1	60.2	134.9	81.1	95.6	89.2	103.7	97.9
11	27.6[c]	24.8	52.4	68.5	161.8	95.0	119.8	90.9	115.7	111.7 (**COP^{II}-18**)
12/13	27.6[c]	24.5	52.1	48.9	122.3	89.1	113.6	85.5	110.0	110.1 (**COP^{II}-19**)
14	27.6[c]	10.1	37.7	46.0	102.1	66.5	76.6	64.4	74.5	72.5 (**COP^{II}-20**)
18	27.6[c]	14.4	42.0	66.9	148.2	71.7	86.1	87.0	101.4	98.2 (**COP^{II}-23**)

[a]R = H for dialdehyde **2** was used in the calculations. [b]R = H for triamine **8** was used in the calculations. [c]Hydrogen instead of $C_{14}H_{29}$ alkyl chain for triamine **9** was used in the calculations.

with larger physical dimensions, the pyramidal triamine **9** was utilized as the top/bottom building blocks to construct elongated triangular bipyramid. Stang and co-workers have reported the self-assembly of similar coordination cages with D_{3h} symmetry from 1,8-bis(*trans*-Pt(PEt_3)$_2$(NO_3))anthracene and tritopic pyridyl subunits (e.g., tris(4-pyridyl)methanol) with 109.5° between the two pyridyl binding sites.[62] Comparable to the successful formation of Stang's D_{3h} supramolecular cages, we were able to obtain **COP^{II}-23** from 1,8-diformylanthracene (**7**) and pyramidal triamine **9** in a decent yield (69%). The formation of the elongated triangular bipyramid using triamine **9**, which has 109.5° angle between any two aryl amines, as the two end-caps requires the angle between the two formyl groups of the dialdehyde connector to be 39°. However, interestingly, in 1,8-diformylanthracene (**7**), the two aldehyde moieties are parallel to each other with the angle of 0°, which is not a perfect match to the required angle of 39°. To further probe the range of angles between two aldehyde moieties of the same building block that allows the successful COP formation, we tested dialdehydes **1** and **4** with 60° angle, **5** with 180° angle, and **2a**-**b** with 300° angle, in the imine condensation/metathesis with triamine **9**. Covalent assembly of dialdehyde **1** with triamine **9** provided the desired molecular cage **COP^{II}-18** in a good yield (78%). Similarly, the reaction between *o*-phenyleneethynylene-based dialdehyde **4** and triamine **9** also provided an excellent yield (94%) of **COP^{II}-21** (entry 15). However, reactions between dialdehyde **5** with a 180° angle, or dialdehyde **2a**−**b** with a 300° angle between the two aldehyde groups, and triamine **9** afforded only a trace amount, if any, of target COPs. The experimental results suggest the COP formation is tolerant to some degree of geometry mismatch. However, significant mismatch would cause energy penalty and prevent the formation of COP products. The preferential formation of target COPs is expected when building blocks have least geometry mismatch and hence least strain. In the assembly of trigonal prisms, since the angle between the two triangular faces of the target trigonal prisms is 0°, ideal dialdehyde connectors should have the angle between the two aldehyde groups close to 0°. Satisfying such geometrical requirement, dialdehydes **6** and **7** with 0° angle between the two aldehyde groups formed prismatic cages (**COP^{I}-16a**, **16b**, **17a**) with planar triamine **8b**. However, imine condensation/metathesis of **8b** with dialdehydes (**1**, **3**, and **4**) bearing 60° angle between the two aldehyde moieties resulted in partially closed intermediates (i.e., I_2, or I_3) without any noticeable amount of the desired COP structures, presumably due to the "misalignment" of amine and aldehyde functional groups. Compared to the planar triamine **8b**, pyramidal triamine **9** appears to be slightly more conformationally flexible and more tolerant to the geometry mismatch with the dialdehyde counterparts.

In addition to the angular effect on the covalent assembly process, we found the conformational rigidity of the building blocks can also influence the outcome of the self-assembly. Dialdehydes **3** and **6** have multiple pseudo *trans*/*cis* conformational isomers, which arise from the free rotation of aryl moieties along the acetylene axis. This conformational flexibility showed negative effect on the formation of COPs, for example, entry 11 (**COP^{II}-18**, 78%) versus entry 14 (**COP^{II}-20**, 31%). The two aldehyde groups of **1** in entry 11 are directionally locked with a favorable 60° angle between them, a preorganization greatly facilitating the COP formation. However, in **3** (entry 14), two planar conformational isomers exist in which the two formyl groups may form a 60° (pseudo-*cis*) or 180° (pseudo-*trans* conformation) angle. Due to the angle mismatch, the pseudo-*trans* isomer would promote the oligomer/polymer side product formation. Therefore, the yield difference in entry 11 and 14 could be attributed to the better functional group directionality in dialdehyde **1**. To support such a rationale, dialdehyde **4** that has the same distance and angle between the two aldehyde groups as in compound **3** but with better directionality (i.e., two aldehydes groups are locked into one conformation) was utilized, and the reaction indeed provided a much higher yield (94%) of the cage product. Such a notion is further supported by the comparison of entries 8 and 9 (**COP^{II}-16b**, 46% vs **COP^{I}-17a**, 74%) and also entries 17 and 18 (**COP^{II}-22**, 11% vs **COP^{II}-23** 69%). These results demonstrate the importance of functional group orientation (directionality) and rigidity in the molecular cage formation.

Solubility Concern. It should be noted that good solubility of the building blocks and reaction intermediates is critical to successful formation of COPs through the dynamic covalent chemistry. Solvent selection thus appears to be one important factor. Attempted formation of **COP^{II}-18** in $CHCl_3$ resulted in a large amount of precipitates and provided a complex mixture of intermediates. In great contrast, reaction in 1,2,4-trichlorobenzene (TCB), in which dialdehyde **1** has a better solubility, provided a good yield of **COP^{II}-18** (78%, entry 11). Although Warmuth et al. have reported the formation of different nanocage products in different solvents, we did not observe such a solvent effect.[63] Another interesting observation possibly related to the poor solubility issue is the low-yielding syntheses of **COP^{I}-15a** (23%) and **COP^{I}-16a** (21%), the structural analogues of **COP^{I}-15b** and **COP^{I}-16b**, respectively. The dialdehydes **2a** and **6a** bear no solubilizing chains, and we observed a significant amount of precipitation during the assembly process presumably due to the low solubility of the reaction intermediates and polymer side products. Therefore,

dx.doi.org/10.1021/jo3011683 | J. Org. Chem. 2012, 77, 7392−7400

when utilizing dynamic covalent chemistry, usually a good solubility of the intermediate products needs to be maintained to ensure high-yielding product formation.

Computational Study. In the COP synthesis via a dynamic covalent approach, the product distribution is determined by the thermodynamic stability of each possible product at the equilibrium. A large energy gap is required in order to obtain predominant target structure over other possible products. In order to illustrate that the energy gap principle accounts for the high yield of the COP product, we performed simple calculations on the energies of the building blocks (triamines III and dialdehydes IV), three possible intermediates (I_2, I_4, and I_5), and COPs. The energies of the selected reaction intermediates along the pathway to COPs, consisting of covalent energies (bond, angle, and torsion) and noncovalent energies (vdW and electrostatic), were calculated at the molecular mechanics level and are listed in Table 2. The covalent interactions in MM are treated as "strings" so that the energies at the equilibrium position are always zero. To make the energy comparison easier, for building blocks and intermediates, the oxygen atom in -CHO or the two hydrogen atoms in -NH_2 were not included. In this way, intermediates and COPs can be constructed with individual building blocks. By comparing the energies of COPs (or intermediates) with ones of corresponding building blocks, the "strain" energy in molecules was estimated. For each entry, energies of structures I_5 + I_5 + IV, I_4 + IV, and I_2 + IV that contain the same number of building blocks as a COP, two molecules of triamines and three molecules of dialdehydes, were compared to the energy of the desired COP product. Consistent with the experimental results, in entries 2, 11, and 14, the COP products are thermodynamically favored and are the predominant species at the equilibrium. In entries 1, 4, 5, 12, and 13, the corresponding COP products do not have significantly lower energies compared to other species, and the reaction did not yield the target COPs as the predominant and isolable species. In entry 18, intermediate I_4 + IV has lower energy than the corresponding COP. Therefore, the unexpected formation of COP product could be kinetically determined.

It should be noted that introducing some degree of rotational freedom into the building blocks could substantially release the angle strain in the COPs and increase their thermodynamic stabilities. For example, the aldehyde moieties in dialdehyde **2** have some degree of flexibility through the aryl−aryl single bond rotation, whereas in dialdehyde **1**, the angle is locked to 60°. This slight difference in the structure significantly reduces the angle strain and lowers the energies of the corresponding COPs by 21 kcal/mol from 139.6 (entry 1) to 117.6 kcal/mol (entry 2/3). Therefore, when dialdehyde **2** and **1** reacted with the same triamine **8b**, respectively, **2** formed **COP^{I}-15a/b** (entry 2/3), while **1** failed to form the cage (entry 1). The results suggest introduction of slight conformational flexibility in the building block design could minimize the buildup of angle strains during the assembly process without greatly sacrificing the benefit from the rigidity of the building blocks.

SUMMARY

A series of imine condensation/metathesis reactions between planar or pyramidal triamines and dialdehydes was conducted to explore the critical structural elements required for the successful shape-persistent COP formation. The experimental results showed that both the angle and the directionality (e.g., two aldehyde groups locked in the same direction) of the functional groups as well as their solubility in the reaction medium are very important. The alignment of aldehyde and amino groups in the precursors with an appropriate angle is highly desired. The presence of certain rotational freedom in the building blocks can decrease the angle strain built along the cage formation, thus facilitating the cage synthesis. The football-shaped molecular cage **COP^{II}-20** shows a high ideal selectivity in adsorption of CO_2 over N_2 (80/1, v/v), thus showing great potential, together with other recently developed COPs, for carbon capture applications.

EXPERIMENTAL SECTION

Compound 1. Compound **10** (33.8 mg, 0.135 mmol), 4-iodobenzaldehyde (126 mg, 0.54 mmol), CuI (0.52 mg, 0.003 mmol), and $Pd(PPh_3)_2Cl_2$ (5.7 mg, 0.008 mmol) were placed in a 25-mL Schlenk tube. The mixture was degassed by evacuating and refilling with nitrogen three times. THF (3.4 mL) and piperidine (0.05 mL) were added, and the mixture was stirred at rt for 18 h. The crude reaction mixture was then concentrated, and the residue was purified by flash column chromatography (CH_2Cl_2) to provide compound **1** as a yellow solid (73 mg, 100%): ^{1}H NMR (400 MHz, $CDCl_3$) δ 10.08 (s, 2H), 8.79 (s, 2H), 8.26 (d, J = 8.0 Hz, 2H), 8.20 (d, J = 8.0 Hz, 2H), 8.12 (s, 2H), 8.01−7.93 (m, 4H), 7.92−7.83 (m, 4H); ^{13}C NMR (75 MHz, $CDCl_3$) δ 191.6, 135.8, 132.4, 132.3, 132.1, 130.5, 130.0, 129.9, 128.6, 126.8, 125.7, 124.4, 118.1, 95.1, 92.7; HR-MS (ESI) calcd for $C_{34}H_{18}O_2$ [M + Li^+] 465.1468, found 465.1470.

Compound 2a. The general procedure for Sonogashira coupling described above was followed. Compound **10** (57 mg, 0.23 mmol) was converted to dialdehyde **2a** using CuI (0.86 mg, 0.005 mmol), $Pd(PPh_3)_2Cl_2$ (10 mg, 0.014 mmol), 3-bromo-5-iodo-benzaldehyde (282 mg, 0.91 mmol), THF (6 mL), and piperidine (0.1 mL). The crude product was purified by flash column chromatography (CH_2Cl_2) to give compound **2a** as an orange solid (34 mg, 24%): ^{1}H NMR (500 MHz, $CDCl_3$) δ 10.04 (s, 2H), 8.78 (s, 2H), 8.29−8.24 (m, 2H), 8.24−8.18 (m, 2H), 8.15 (s, 2H), 8.14 (s, 2H), 8.12 (s, 2H), 8.04 (s, 2H); ^{13}C NMR (75 MHz, $CDCl_3$) δ 190.3, 139.7, 138.1, 132.2, 132.11, 132.07, 131.6, 130.4, 128.6, 126.72, 126.65, 125.7, 124.3, 123.5, 117.7, 92.9, 91.5; HR-MS (ESI) calcd for $C_{34}H_{16}Br_2O_2$ [M + Li^+] 622.9660, found 622.9673.

3-Bromo-5-(1-dodecyn-1-yl)-benzaldehyde. The general procedure for Sonogashira coupling described above was followed. 3-Bromo-5-iodo-benzaldehyde (1.0 g, 3.2 mmol) was converted to 3-bromo-5-(1-dodecyn-1-yl)-benzaldehyde using CuI (6 mg, 0.032 mmol), $Pd(PPh_3)_2Cl_2$ (68 mg, 0.097 mmol), 1-decyen (2.32 mL, 12.9 mmol), THF (38 mL), and piperidine (4 mL). The crude product was purified by flash column chromatography (hexanes → EtOAc) to provide the pure product as a brown liquid (1.05 g, 100%): ^{1}H NMR (500 MHz, $CDCl_3$) δ 9.92 (s, 1H), 7.90 (t, J = 1.7 Hz, 1H), 7.80 (t, J = 1.4 Hz, 1H), 7.77 (t, J = 1.6 Hz, 1H), 2.45−2.39 (m, 3H), 1.65−1.57 (m, 3H), 1.48−1.41 (m, 3H), 1.36−1.25 (m, 13H), 0.90 (t, J = 7.0 Hz, 5H). ^{13}C NMR (75 MHz, $CDCl_3$) δ 190.2, 139.6, 137.6, 131.6, 130.8, 127.2, 122.9, 94.1, 78.1, 31.8, 29.2, 29.1, 28.9, 28.5, 22.7, 19.4, 14.1; HR-MS (ESI) calcd for $C_{17}H_{21}BrO$ [M + H^+] 321.0849, found 321.0849.

Compound 2b. The general procedure for Sonogashira coupling described above was followed. Compound **10** (513 mg, 1.6 mmol) was converted to dialdehyde **2b** using CuI (1.5 mg, 0.008 mmol), $Pd(PPh_3)_2Cl_2$ (17 mg, 0.024 mmol), 3-bromo-5-(1-dodecyn-1-yl)-benzaldehyde (100 mg, 0.40 mmol), and triethylamine (5.5 mL). The crude product was purified by flash column chromatography (50% $CHCl_3$ in hexane → 75% $CHCl_3$ in hexane) to give compound **2b** as an orange solid (173 mg, 59%): ^{1}H NMR (500 MHz, $CDCl_3$) δ 10.05 (s, 2H), 8.81 (s, 2H), 8.28−8.22 (m, 2H), 8.22−8.17 (m, 2H), 8.14−8.09 (m, 4H), 7.99 (t, J = 4.6, 3.1 Hz, 2H), 7.90 (t, 2H), 2.46 (t, 4H), 1.71−1.60 (m, 4H), 1.53−1.44 (m, 4H), 1.38−1.28 (m, 16H), 0.89 (t, J = 7.1 Hz, 6H); ^{13}C NMR (75 MHz, $CDCl_3$) δ 191.2, 139.7, 136.7, 132.4, 131.9, 131.7, 131.3, 130.2, 128.3, 126.5, 126.0, 125.3, 124.9, 124.0, 117.9, 93.8, 93.5, 90.5, 78.9, 32.1, 29.44, 29.36, 29.2, 28.8, 22.9,

dx.doi.org/10.1021/jo3011683 | J. Org. Chem. 2012, 77, 7392−7400

19.7, 14.4; HR-MS (ESI) calcd for $C_{54}H_{50}O_2$ [M^+] 730.3806, found 730.3825.

Compound 12. To a solution of the acid **11** (719 mg, 1.25 mmol) in MeOH (60 mL) was added concentrated H_2SO_4 (0.7 mL). The solution was refluxed for 15 h and cooled to rt. The solvent was evaporated, and water (50 mL) was added. The product was extracted with CH_2Cl_2 (3 × 50 mL). The combined organic extracts were dried over anhydrous Na_2SO_4 and concentrated to give crude product. Purification by flash column chromatography (10% CH_2Cl_2, 8% EtOAc in hexane) provided the methyl ester **12** (600 mg, 77%):^{1}H NMR (400 MHz, $CDCl_3$) δ 8.09−7.80 (m, 6H), 7.72−7.49 (m, 2H), 7.31−7.25 (m, 6H), 7.06−6.83 (m, 2H), 3.92 (s, 9H); ^{13}C NMR (101 MHz, $CDCl_3$) δ 166.8, 150.3, 145.0, 137.4, 132.9, 130.9, 129.5, 128.7, 92.9, 65.4, 52.4. The NMR data were consistent with the literature report by Anderson.[59]

Compound 13. A solution of 1-tetradecene (485 mg, 2.47 mmol) in THF (2 mL) was stirred and cooled to 0 °C. 9-BBN (4.94 mL, 0.5 M solution in THF) was added dropwise, and the solution was slowly warmed to rt. After stirring at rt for 6 h, $Pd(PPh_3)_4$ (95 mg, 0.08 mmol) and K_2CO_3 (453 mg, 3.28 mmol) were added followed by compound **12** (1.02 g, 1.64 mmol) in DMF (5 mL). The mixture was heated at 50 °C for 16 h and then cooled to rt. Water (60 mL) was added, and the reaction mixture was extracted with EtOAc (3 × 60 mL). The combined organic extracts were washed with water (3 × 60 mL) and brine (60 mL), dried over anhydrous Na_2SO_4, and concentrated to give the crude product. The residue was purified by flash column chromatography (10% EtOAc, 10% CH_2Cl_2 in hexane) to give the product **13** as a yellow solid (840 mg, 74%): ^{1}H NMR (400 MHz, $CDCl_3$) δ 7.97−7.89 (m, 6H), 7.33−7.28 (m, 6H), 7.09−7.03 (m, 4H), 3.91 (s, 9H), 2.62−2.52 (m, 2H), 1.65−1.59 (m, 2H), 1.36−1.21 (m, 23H), 0.88 (t, 3H); ^{13}C NMR (75 MHz, $CDCl_3$) δ 166.8, 150.9, 142.0, 141.4, 130.8, 130.6, 129.1, 128.2, 128.0, 65.2, 52.1, 35.4, 31.9, 31.3, 29.7, 29.6, 29.49, 29.45, 29.36, 22.7, 14.1; HR-MS (ESI) calcd for $C_{45}H_{54}O_6$ [$M + H^+$] 691.3993, found 691.3986.

Compound 14. To a suspension of compound **13** (2.57 g, 3.72 mmol) in EtOH (40 mL) was added a solution of KOH (3.12 g, 55.8 mmol) in H_2O (12 mL). The mixture was refluxed for 16 h, and cooled to rt. It was then acidified with HCl (1 N, ∼100 mL) and extracted with EtOAc (3 × 100 mL). The combined organic extracts were dried over anhydrous Na_2SO_4, and concentrated to give compound **14** as a colorless solid (2.37 g, 98%): ^{1}H NMR (500 MHz, DMSO) δ 7.92 (d, J = 8.4 Hz, 6H), 7.35 (d, J = 8.5 Hz, 6H), 7.19 (d, J = 8.4 Hz, 2H), 7.11 (d, J = 8.4 Hz, 2H), 1.61−1.51 (m, 2H), 1.28−1.23 (m, 24H), 0.87 (t, J = 6.6 Hz, 3H); ^{13}C NMR (101 MHz, CD_3OD) δ 169.4, 152.4, 143.7, 142.6, 132.0, 131.9, 130.3, 130.0, 129.2, 66.4, 36.4, 33.2, 33.1, 32.5, 30.81, 30.79, 30.7, 30.6, 30.5, 30.4, 27.5, 23.8, 23.1, 14.5; HR-MS (ESI) calcd for $C_{42}H_{48}O_6$ [$M - H^-$] 647.3378, found 647.3380.

Compound 9. Step 1: A solution of compound **14** (2.37 g, 3.65 mmol) in CH_2Cl_2 (20 mL) and THF (5 mL) was stirred and cooled at 0 °C. Oxalyl chloride (4.17 g, 32.9 mmol) was added dropwise, followed by DMF (3 drops) at 0 °C. The mixture was allowed to warm to rt and stirred for 1 h. TLC showed all the compound **14** was consumed. The volatiles were evaporated to give light yellow solid (2.71 g), which was used in the following step without further purification.

Step 2: A solution of the above acyl chloride (2.71 g) in acetone (100 mL) was stirred and cooled to 0 °C, as a solution of NaN_3 (2.14 g, 32.9 mmol) in H_2O (10 mL) was added dropwise. The mixture was stirred at 0 °C for 1 h. The solvent was evaporated and water (50 mL) was added. The organic was separated, and the aqueous layer was extracted with Et_2O (5 × 50 mL). The combined organic extracts were dried over anhydrous Na_2SO_4 and concentrated to give the crude product (3.05 g), which was used in the following step without further purification

Step 3: To the solution of the above acyl azide (3.05 g) in toluene (40 mL) was added benzyl alcohol (3.55 g, 32.9 mmol). The solution was refluxed for 2 h, at which point TLC showed complete conversion of the acyl azide to carbamate. Ethyl acetate (150 mL) was added, and the solution was washed with saturated $NaHCO_3$ (2 × 100 mL) and brine (100 mL), dried over anhydrous Na_2SO_4, and concentrated to give the crude product, which contained excess benzyl alcohol. It was directly hydrolyzed without further purification.

Step 4: To the solution of the above carbamate in EtOH (40 mL) was added a solution of KOH (3.07 g, 54.98 mmol) in H_2O (4 mL). The mixture was heated at 95 °C for 18 h. The volatiles were removed and water (100 mL) was added. The product was extracted with Et_2O (3 × 80 mL). The combined ethereal extracts were washed with brine (150 mL), dried over Na_2SO_4, and concentrated to give the crude product as a pink oil. Purification by flash column chromatography (20% EtOAc in hexane → 8% MeOH in CH_2Cl_2) provided the amine **9** as a light yellow solid (1.20 g, 57% in four steps): ^{1}H NMR (500 MHz, $CDCl_3$) δ 7.07 (d, J = 8.4 Hz, 2H), 7.01 (d, J = 8.4 Hz, 2H), 6.97−6.93 (m, 6H), 6.58−6.54 (m, 6H), 3.58 (s, 6H), 2.59−2.49 (m, 2H), 1.63−1.57 (m, 2H), 1.35−1.20 (m, 24H), 0.89 (t, J = 6.9 Hz, 3H); ^{13}C NMR (75 MHz, $CDCl_3$) δ 145.4, 144.0, 140.1, 138.4, 132.2, 131.1, 127.3, 114.2, 62.7, 35.7, 32.2, 31.6, 29.92, 29.88, 29.84, 29.76, 29.7, 29.6, 22.9, 14.4; HR-MS (ESI) calcd for $C_{39}H_{51}N_3$ [$M + H^+$] 562.4156, found 562.4159.

General Procedure for COP Synthesis. To a solution of **8b** (20 mg, 0.032 mmol) and **2a** (30 mg, 0.049 mmol) in 1,2,4-trichlorobenzene (TCB) (11 mL) was added a solution of TFA (0.38 μL, 0.0049 mmol) in $CHCl_3$ (100 μL) slowly dropwise. The solution was stirred at rt for 18 h, at which time ^{1}H NMR spectrum of the concentrated crude reaction mixture indicated both of the starting materials were consumed. DIBAL-H (960 μL, 0.96 mmol, 1.0 M in CH_2Cl_2) was added. After stirring at rt for 20 min, the reaction was quenched with MeOH (1 mL), and saturated $NaHCO_3$ (15 mL) was added. The mixture was stirred at rt for 30 min, and the organic layer was separated. The aqueous solution was extracted with $CHCl_3$ (3 × 30 mL). The combined organics were dried over Na_2SO_4 and concentrated to give the crude product. Purification by flash column chromatography (CH_2Cl_2) provided the pure product **COP-15a** as a yellow solid (11 mg, 23%): ^{1}H NMR (500 MHz, THF) δ 8.79 (br s, 6H), 8.25 (br s, 12H), 8.15 (br s, 6H), 7.82 (s, 3H), 7.77 (s, 3H), 7.66 (s, 3H), 7.01−6.80 (m, 12H), 6.78−6.49 (m, 12H), 5.53−5.13 (m, 6H), 4.33 (d, J = 4.8 Hz, 12H), 2.17−2.10 (m, 4H), 1.35−0.74 (m, 56H), 0.69 (t, J = 7.3 Hz, 18H); ^{13}C NMR (75 MHz, THF) δ 148.0, 144.7, 140.6, 140.4, 133.6, 133.0, 132.9, 132.1, 131.9, 131.8, 131.0, 130.7, 129.3, 127.4, 126.5, 126.4, 125.2, 123.2, 119.2, 113.1, 95.3, 90.3, 48.7, 33.1, 32.0, 31.3, 30.8, 30.6, 30.5, 30.0, 23.7, 23.3, 14.8, 14.6; MS (MALDI) calcd for $C_{186}H_{162}Br_6N_6$ ([M^+]) 2960.80, found 2960.75.

COP^{I}-15b. The general procedure for COP synthesis described above was followed. Compound **8b** (11 mg, 0.018 mmol) and **2b** (20 mg, 0.027 mmol) were converted to **COP^{I}-15b** (25 mg, 83%, a yellow solid) using TFA (0.21 μL, 0.0027 mmol), $CHCl_3$ (6 mL), and DIBAL-H (540 μL, 0.54 mmol, 1.0 M in CH_2Cl_2, 0 °C). The physical data for **COP^{I}-15b**: ^{1}H NMR (500 MHz, $CDCl_3$) δ 8.79 (br s, 6H), 8.24−8.19 (m, 6H), 8.18−8.14 (m, 6H), 8.09 (s, 6H), 7.80 (br s, J = 13.1 Hz, 6H), 7.68 (br s, 6H), 7.48 (br s, J = 8.8 Hz, 6H), 7.16 (br s, 6H), 6.68 (s, 18H), 4.29 (s, 12H), 3.81 (s, 6H), 2.44 (t, J = 7.1 Hz, 12H), 2.17−2.07 (m, 12H), 1.66−1.60 (m, 12H), 1.51−1.45 (m, 12H), 1.38−1.24 (m, 72H), 1.24−1.15 (m, 12H), 1.06−1.00 (m, 12H), 0.89 (t, J = 6.8 Hz, 18H), 0.76 (t, J = 7.3 Hz, 18H); ^{13}C NMR (75 MHz, $CDCl_3$) δ 146.4, 140.1, 139.9, 139.2, 133.9, 132.2, 132.0, 131.7, 131.3, 130.8, 128.3, 126.8, 125.4, 125.1, 124.4, 124.1, 118.6, 112.8, 95.3, 91.8, 89.2, 80.0, 49.1, 32.1, 31.2, 29.9, 29.8, 29.5, 29.4, 29.2, 29.0, 22.9, 22.6, 19.7, 14.44, 14.36; MS (MALDI) calcd for $C_{246}H_{264}N_6$ ([M^+]) 3304.09, found 3304.04.

COP^{II}-18. The general procedure for COP synthesis described above was followed. Compound **9** (15 mg, 0.027 mmol) and compound **1** (18 mg, 0.040 mmol) were converted to **COP^{II}-18** (a light yellow solid, 25 mg, 78%) using TFA (0.31 μL, 0.004 mmol), $CHCl_3$ (9 mL), and DIBAL-H (810 μL, 0.81 mmol, 1.0 M in CH_2Cl_2). The physical data for **COP^{II}-18**: ^{1}H NMR (500 MHz, $CDCl_3$) δ 8.98 (s, 6H), 8.10 (d, J = 14.6 Hz, 6H), 7.69 (d, J = 9.0 Hz, 6H), 7.62 (d, J = 13.1 Hz, 6H), 7.57 (d, J = 8.0 Hz, 12H), 7.52 (d, J = 8.2 Hz, 6H), 7.36 (d, J = 8.7 Hz, 12H), 7.12−7.09 (d, 6H), 7.07 (d, J = 7.9 Hz, 12H), 6.37 (d, J = 13.7 Hz, 12H), 3.85 (br s, 12H), 3.22 (br s, 6H), 2.58−2.45 (m, 4H), 1.61−1.54 (m, 4H), 1.37−1.15 (m, 44H), 0.92 (t,

dx.doi.org/10.1021/jo3011683 | J. Org. Chem. 2012, 77, 7392−7400

J = 6.9 Hz, 6H); ^{13}C NMR (101 MHz, Toluene) δ 147.0, 146.7, 141.5, 140.5, 138.6, 138.2, 137.6, 133.01, 133.0, 132.6, 132.3, 132.2, 130.4, 128.2, 128.0, 127.4, 125.4, 123.2, 119.8, 112.8, 96.8, 89.5, 63.8, 48.9, 32.7, 32.1, 30.6, 30.50, 30.48, 30.4, 30.3, 30.2, 23.4; MS (MALDI) calcd for $C_{180}H_{156}N_6$ ([M$^+$]) 2402.24, found 2401.33.

COP^{II}-20. The general procedure for COP synthesis described above was followed. Compound **9** (500 mg, 0.89 mmol) and **3** (313 mg, 1.33 mmol) were converted to **COP^{II}-20** (239 mg, 31%, a light yellow solid) using $Sc(OTf)_3$ (66 mg, 0.13 mmol), $CHCl_3$ (300 mL), and $NaBH(OAc)_3$ (5.66 g, 26.7 mmol). The physical data for **COP^{II}-20**: ^{1}H NMR (500 MHz, $CDCl_3$) δ 7.57 (s, 6H), 7.44−7.40 (m, 6H), 7.32−7.29 (m, 12H), 7.13−7.07 (m, 4H), 7.06−6.99 (m, 4H), 6.95 (br d, J = 8.8 Hz, 12H), 6.49 (br d, J = 7.5 Hz, 12H), 4.29 (s, 12H), 4.00 (s, 6H), 2.59−2.53 (m, 4H), 1.64−1.58 (m, 4H), 1.33−1.24 (m, 44H), 0.89 (t, J = 8.6 Hz, 6H); ^{13}C NMR (75 MHz, $CDCl_3$) δ 145.7, 145.6, 140.3, 140.0, 137.6, 132.2, 131.1, 130.9, 130.4, 128.8, 127.6, 127.2, 123.7, 111.9, 89.7, 62.6, 48.4, 35.7, 32.2, 31.6, 29.93, 29.89, 29.85, 29.78, 29.7, 29.6, 22.9, 14.4; MS (MALDI) calcd for $C_{126}H_{132}N_6$ ([M$^+$]) 1730.05, found 1729.48.

COP^{II}-21. The general procedure for COP synthesis described above was followed. Compound **9** (20 mg, 0.036 mmol) and compound **4** (18 mg, 0.054 mmol) were converted to **COP^{II}-21** (a light yellow solid, 34 mg, 94%) using TFA (0.42 μL, 0.005 mmol), $CHCl_3$ (12 mL), and DIBAL-H (1.08 mL, 1.08 mmol, 1.0 M in CH_2Cl_2). The physical data for **COP^{II}-21**: ^{1}H NMR (500 MHz, $CDCl_3$) δ 7.56 (dd, J = 5.8, 3.4 Hz, 6H), 7.54 (d, J = 8.2 Hz, 12H), 7.33 (d, J = 8.6 Hz, 12H), 7.31 (dd, J = 6.1, 2.7 Hz, 6H), 7.10 (d, J = 8.2 Hz, 4H), 7.04−6.96 (m, 16H), 6.52 (d, J = 8.6 Hz, 12H), 4.27 (s, 12H), 3.92 (s, 6H), 2.60−2.50 (m, 4H), 1.67−1.52 (m, 4H), 1.39−1.19 (m, 44H), 0.89 (t, J = 7.0 Hz, 6H); ^{13}C NMR (75 MHz, $CDCl_3$) δ 145.8, 145.5, 140.3, 140.1, 137.7, 132.2, 132.1, 131.7, 131.1, 128.2, 127.9, 127.3, 126.3, 122.4, 111.9, 93.8, 88.6, 62.6, 48.7, 35.7, 32.2, 31.6, 29.93, 29.89, 29.85, 29.77, 29.75, 29.6, 22.9, 14.4; MS (MALDI) calcd for $C_{150}H_{144}N_6$ ([M$^+$]) 2030.15, found 2030.32.

COP^{II}-22. The general procedure for COP synthesis described above was followed. Compound **9** (49 mg, 0.087 mmol) and compound **6b** (96 mg, 0.130 mmol) were converted to **COP^{II}-22** (a light yellow solid, 15 mg, 11%) using TFA (1.0 μL, 0.013 mmol), $CHCl_3$ (30 mL), and DIBAL-H (2.61 mL, 2.61 mmol, 1.0 M in CH_2Cl_2). The physical data for **COP^{II}-22**: ^{1}H NMR (500 MHz, $CDCl_3$) δ 7.51 (s, 6H), 7.41 (br s, J = 10.8 Hz, 6H), 7.36 (s, 6H), 7.24 (br s, J = 19.8 Hz, 3H), 7.09 (br d, J = 7.7 Hz, 4H), 7.03−6.93 (m, 22H), 6.45 (d, J = 7.3 Hz, 12H), 4.24 (d, J = 25.1 Hz, 12H), 3.96 (app t, J = 6.4 Hz, 12H), 2.55−2.48 (m, 4H), 1.86−1.68 (m, 4H), 1.59−1.50 (m, 4H), 1.47−1.41 (m, 4H), 1.32−1.22 (m, 120H), 0.90−0.87 (m, 15H); ^{13}C NMR (101 MHz, $CDCl_3$) δ ^{13}C NMR (101 MHz, $CDCl_3$) δ 159.1, 145.3, 142.6, 140.2, 137.8, 135.2, 133.1, 132.1, 131.1, 130.7, 129.4, 127.8, 127.3, 125.1, 124.2, 122.5, 118.1, 112.1, 89.9, 88.5, 68.6, 47.7, 35.7, 32.2, 31.6, 29.94, 29.90, 29.86, 29.8, 29.8, 29.6, 29.4, 26.2, 22.9, 14.37; MS (MALDI) calcd for $C_{198}H_{235}Br_6N_6O_3$ ([MH$^+$]) 3226.34, found 3226.71

COP^{II}-23. The general procedure for COP synthesis described above was followed. Compound **9** (45 mg, 0.080 mmol) and **7** (28 mg, 0.120 mmol) were converted to **COP^{II}-23** (48 mg, 69%, a yellow solid) using TFA (0.92 μL, 0.012 mmol), $CHCl_3$ (27 mL), and DIBAL-H ((2.43 mL, 2.43 mmol, 1.0 M in CH_2Cl_2, −40 °C). The physical data for **COP^{II}-23**: ^{1}H NMR (500 MHz, $CDCl_3$) δ 9.03 (s, 3H), 8.49 (s, 3H), 7.98 (d, J = 8.5 Hz, 6H), 7.53 (d, J = 6.6 Hz, 6H), 7.43 (dd, J = 8.3, 6.9 Hz, 6H), 7.12 (d, J = 8.1 Hz, 4H), 7.06−6.98 (m, 16H), 6.52 (d, J = 16.6 Hz, 12H), 4.74 (s, 12H), 3.91 (br s, J = 54.6 Hz, 6H), 2.56 (dd, J = 20.9, 13.2 Hz, 4H), 1.58 (quint, J = 14.7, 7.2 Hz, 4H), 1.32−1.26 (m, 48H), 0.89 (t, J = 6.9 Hz, 6H); ^{13}C NMR (101 MHz, $CDCl_3$) δ 146.3, 145.8, 139.9, 137.5, 135.8, 132.3, 132.2, 131.2, 130.2, 128.6, 127.9, 127.2, 126.5, 125.4, 120.0, 111.7, 62.6, 48.1, 35.7, 32.1, 31.6, 29.92, 29.88, 29.84, 29.77, 29.6, 22.9, 14.4; MS (MALDI) calcd for $C_{126}H_{133}N_6$ ([MH$^+$]) 1731.05, found 1731.15

■ ASSOCIATED CONTENT

Ⓢ Supporting Information

Materials and general synthetic methods, GPC graphs, computational method, and NMR spectra of compounds. This material is available free of charge via the Internet at http://pubs.acs.org.

■ AUTHOR INFORMATION

Corresponding Author

*E-mail: wei.zhang@colorado.edu.

Notes

The authors declare no competing financial interest.

■ ACKNOWLEDGMENTS

We thank Dr. Bret Voss for gas adsorption measurement, National Science Foundation (DMR-1055705) for funding support. Acknowledgment is also made to the donors of the American Chemical Society Petroleum Research Fund for partial support of this research. This research used capabilities of the National Renewable Energy Laboratory Computational Science Center, which is supported by the Office of Energy Efficiency and Renewable Energy of the U.S. Department of Energy under Contract No. DE-AC36-08GO28308.

■ REFERENCES

(1) Cram, D. J. *Nature* **1992**, *356*, 29−36.
(2) Hof, F.; Craig, S. L.; Nuckolls, C.; Rebek, J., Jr. *Angew. Chem., Int. Ed.* **2002**, *41*, 1488−1508.
(3) Seidel, S. R.; Stang, P. J. *Acc. Chem. Res.* **2002**, *35*, 972−983.
(4) Fujita, M.; Tominaga, M.; Hori, A.; Therrien, B. *Acc. Chem. Res.* **2005**, *38*, 369−378.
(5) Biros, S. M.; Rebek, J. *Chem. Soc. Rev.* **2007**, *36*, 93−104.
(6) Dalgarno, S. J.; Power, N. P.; Atwood, J. L. *Coord. Chem. Rev.* **2008**, *252*, 825−841.
(7) Jin, P.; Dalgarno, S. J.; Atwood, J. L. *Coord. Chem. Rev.* **2010**, *254*, 1760−1768.
(8) Lehn, J. M.; Eliseev, A. V. *Science* **2001**, *291*, 2331−2332.
(9) Rowan, S. J.; Cantrill, S. J.; Cousins, G. R. L.; Sanders, J. K. M.; Stoddart, J. F. *Angew. Chem., Int. Ed.* **2002**, *41*, 898−952.
(10) Sanders, J. K. M.; Corbett, P. T.; Leclaire, J.; Vial, L.; West, K. R.; Wietor, J. L.; Otto, S. *Chem. Rev.* **2006**, *106*, 3652−3711.
(11) Lehn, J. M. *Chem. Soc. Rev.* **2007**, *36*, 151−160.
(12) Rebek, J., Jr. *Angew. Chem., Int. Ed.* **2005**, *44*, 2068−2078.
(13) Bisson, A. P.; Lynch, V. M.; Monahan, M. K. C.; Anslyn, E. V. *Angew. Chem., Int. Ed.* **1997**, *36*, 2340−2342.
(14) Ferrand, Y.; Crump, M. P.; Davis, A. P. *Science* **2007**, *318*, 619−22.
(15) Sarmentero, M. A.; Fernandez-Perez, H.; Zuidema, E.; Bo, C.; Vidal-Ferran, A.; Ballester, P. *Angew. Chem., Int. Ed.* **2010**, *49*, 7489−7492.
(16) Inokuma, Y.; Kawano, M.; Fujita, M. *Nat. Chem.* **2011**, *3*, 349−358.
(17) Dawn, S.; Dewal, M. B.; Sobransingh, D.; Paderes, M. C.; Wibowo, A. C.; Smith, M. D.; Krause, J. A.; Pellechia, P. J.; Shimize, L. S. *J. Am. Chem. Soc.* **2011**, *133*, 7025−7032.
(18) Hastings, C. J.; Backlund, M. P.; Bergman, R. G.; Raymond, K. N. *Angew. Chem., Int. Ed.* **2011**, *50*, 10570−10573.
(19) Tozawa, T.; Jones, J. T. A.; Swamy, S. I.; Jiang, S.; Adams, D. J.; Shakespeare, S.; Clowes, R.; Bradshaw, D.; Hasell, T.; Chong, S. Y.; Tang, C.; Thompson, S.; Parker, J.; Trewin, A.; Bacsa, J.; Slawin, A. M. Z.; Steiner, A.; Cooper, A. I. *Nat. Mater.* **2009**, *8*, 973−978.
(20) Atwood, J. L.; Barbour, L. J.; Jerga, A. *Science* **2002**, *296*, 2367−2369.
(21) Jin, Y. H.; Voss, B. A.; Jin, A.; Long, H.; Noble, R. D.; Zhang, W. *J. Am. Chem. Soc.* **2011**, *133*, 6650−6658.

(22) Bergman, R. G.; Fiedler, D.; Leung, D. H.; Raymond, K. N. *Acc. Chem. Res.* **2005**, *38*, 349−358.
(23) MacGillivray, L. R.; Atwood, J. L. *Angew. Chem., Int. Ed.* **1999**, *38*, 1019−1034.
(24) Evan-Salem, T.; Baruch, I.; Avram, L.; Cohen, Y.; Palmer, L. C.; Rebek, J. *Proc. Natl. Acad. Sci. U.S.A.* **2006**, *103*, 12296−12300.
(25) Liu, S.; Gibb, B. C. *Chem. Commun.* **2008**, 3709−3716.
(26) Ajami, D.; Rebek, J., Jr. *Nat. Chem.* **2009**, *1*, 87−90.
(27) Ward, M. D.; Liu, Y. Z.; Hu, C. H.; Comotti, A. *Science* **2011**, *333*, 436−440.
(28) Meyer, C. D.; Joiner, C. S.; Stoddart, J. F. *Chem. Soc. Rev.* **2007**, *36*, 1705−1723.
(29) Mastalerz, M. *Angew. Chem., Int. Ed.* **2010**, *49*, 5042−5053.
(30) Belowich, M. E.; Valente, C.; Stoddart, J. F. *Angew. Chem., Int. Ed.* **2010**, *49*, 7208−7212.
(31) Holst, J. R.; Trewin, A.; Cooper, A. I. *Nat. Chem.* **2010**, *2*, 915−920.
(32) Hasell, T.; Wu, X. F.; Jones, J. T. A.; Bacsa, J.; Steiner, A.; Mitra, T.; Trewin, A.; Adams, D. J.; Cooper, A. I. *Nat. Chem.* **2010**, *2*, 750−755.
(33) Jin, Y. H.; Voss, B. A.; Noble, R. D.; Zhang, W. *Angew. Chem., Int. Ed.* **2010**, *49*, 6348−6351.
(34) Rue, N. M.; Sun, J. L.; Warmuth, R. *Isr. J. Chem.* **2011**, *51*, 743−768.
(35) Nishimura, N.; Kobayashi, K. *Angew. Chem., Int. Ed.* **2008**, *47*, 6255−6258.
(36) Christinat, N.; Scopelliti, R.; Severin, K. *Angew. Chem., Int. Ed.* **2008**, *47*, 1848−1852.
(37) Naumann, C.; Place, S.; Sherman, J. C. *J. Am. Chem. Soc.* **2002**, *124*, 16−17.
(38) West, K. R.; Bake, K. D.; Otto, S. *Org. Lett.* **2005**, *7*, 2615−2618.
(39) Zhang, C.-X.; Long, H.; Zhang, W. *Chem. Commun.* **2012**, *48*, 6172−6174.
(40) Zhang, C.; Wang, Q.; Long, H.; Zhang, W. *J. Am. Chem. Soc.* **2011**, *133*, 20995−21001.
(41) Jin, Y. H.; Voss, B. A.; McCaffrey, R.; Baggett, C. T.; Noble, R. D.; Zhang, W. *Chem. Soc.* **2012**, *3*, 874−877.
(42) Sircar, A.; Myers, A. L. *Gas Seperation by Zeolites*; Dekker: New York, 2003.
(43) Yu, M.; Noble, R. D.; Falconer, J. L. *Acc. Chem. Res.* **2011**, *44*, 1196−1206.
(44) Li, J. R.; Kuppler, R. J.; Zhou, H. C. *Chem. Soc. Rev.* **2009**, *38*, 1477−1504.
(45) Wang, Z. Q.; Cohen, S. M. *Chem. Soc. Rev.* **2009**, *38*, 1315−1329.
(46) Long, J. R.; Yaghi, O. M. *Chem. Soc. Rev.* **2009**, *38*, 1213−1214.
(47) Furukawa, H.; Ko, N.; Go, Y. B.; Aratani, N.; Choi, S. B.; Choi, E.; Yazaydin, A. O.; Snurr, R. Q.; O'Keeffe, M.; Kim, J.; Yaghi, O. M. *Science* **2010**, *329*, 424−428.
(48) Farha, O. K.; Hupp, J. T. *Acc. Chem. Res.* **2010**, *43*, 1166−1175.
(49) Cote, A. P.; Benin, A. I.; Ockwig, N. W.; O'Keeffe, M.; Matzger, A. J.; Yaghi, O. M. *Science* **2005**, *310*, 1166−1170.
(50) Mastalerz, M. *Angew. Chem., Int. Ed.* **2008**, *47*, 445−447.
(51) Qiu, S. L.; Ben, T.; Ren, H.; Ma, S. Q.; Cao, D. P.; Lan, J. H.; Jing, X. F.; Wang, W. C.; Xu, J.; Deng, F.; Simmons, J. M.; Zhu, G. S. *Angew. Chem., Int. Ed.* **2009**, *48*, 9457−9460.
(52) Doonan, C. J.; Tranchemontagne, D. J.; Glover, T. G.; Hunt, J. R.; Yaghi, O. M. *Nat. Chem.* **2010**, *2*, 235−238.
(53) Colson, J. C., J. W.; Woll, A. R.; Mukherjee, A.; Levendorf, M. P.; Spitler, E. L.; Shields, V. B.; Spencer, M. G.; Park, J.; Dichtel, W. R. *Science* **2011**, *332*, 228−231.
(54) Tian, J.; Thallapally, P. K.; Dalgarno, S. J.; McGrail, P. B.; Atwood, J. L. *Angew. Chem., Int. Ed.* **2009**, *48*, 5492−5495.
(55) Thallapally, P. K.; Tian, J.; Ma, S. Q.; Fowler, D.; McGrail, B. P.; Atwood, J. L. *Chem. Commun.* **2011**, *47*, 7626−7628.
(56) Mastalerz, M.; Schneider, M. W.; Oppel, I. M.; Presly, O. *Angew. Chem., Int. Ed.* **2011**, *50*, 1046−1051.
(57) Northrop, B. H.; Zheng, Y. R.; Chi, K. W.; Stang, P. J. *Acc. Chem. Res.* **2009**, *42*, 1554−1563.
(58) Ji, S. M.; Yang, J.; Yang, Q.; Liu, S. S.; Chen, M. D.; Zhao, J. Z. *J. Org. Chem.* **2009**, *74*, 4855−4865.
(59) Daniell, H. W.; Klotz, E. J. F.; Odell, B.; Claridge, T. D. W.; Anderson, H. L. *Angew. Chem., Int. Ed.* **2007**, *46*, 6845−6848.
(60) We observed some side reactions in entries 15 and 18, when we reduced the imine-linked COPs at 0 °C. Therefore, reduction of imines with DIBAL-H at lower temperature is recommended.
(61) The CO_2 adsorption capacity of **COP^{II}-20** does not show enhancement compared to the previous reported trigonal prismatic cages.
(62) Kuehl, C. J.; Kryschenko, Y. K.; Radhakrishnan, U.; Seidel, S. R.; Huang, S. D.; Stang, P. J. *Proc. Natl. Acad. Sci. U.S.A.* **2002**, *99*, 4932−4936.
(63) Liu, X. J.; Warmuth, R. *J. Am. Chem. Soc.* **2006**, *128*, 14120−14127.